Article:
Yan, Yu, Lu, Xianyang, Liu, Bo et al. (2020) Element-specific spin and orbital moments and perpendicular magnetic anisotropy in Ta/CoFeB/MgO structures. Journal of Applied Physics. 063903. ISSN: 1089-7550

https://doi.org/10.1063/1.5129489

Element-specific spin and orbital moments and perperndicular magnetic anisotropy in Ta/CoFeB/MgO structures

Yu Yan,[†,‡,△] Xianyang Lu,[†,¶,△] Bo Liu,[†] Xiaoqian Zhang,[†] Xiangyu Zheng,[†,‡] Hao Meng,[§] Wenqing Liu,[*,†,‖] Junlin Wang,[†,‡] Iain G. Will,[‡] Jing Wu,[†,¶] Ping Kwan Johnny Wong,[†,⊥] Jianwang Cai,[*,#] Jun Du,[@] Rong Zhang,[†] and Yongbing Xu[*,†,‡]

†*York-Nanjing Joint Centre (YNJC) for Spintronics and Nano-engineering, School of Electronic Science and Engineering, Nanjing University, Nanjing 210093, China*

‡*Spintronics and Nanodevice laboratory, Department of Electronic Engineering, University of York, YO10 5DD, United Kingdom*

¶*Department of Physics, University of York, YO10 5DD, United Kingdom*

§*Zhejiang Hikstor Technology Company, Hangzhou 311305, China*

‖*Department of Electronic Engineering, Royal Holloway University of London, TW20 0EX, United Kingdom*

⊥*NanoElectronics Group, MESA+ Institute for Nanotechnology, University of Twente, 7500 AE, Enschede, The Netherlands*

#*Institute of Physics, Chinese Academy of Science, Beijing 100190, China*

@*National Laboratory of Solid State Microstructures and Department of Physics, Nanjing University, Nanjing 210093, China*

△*Contributed equally to this work*

E-mail: Wenqing.Liu@rhul.ac.uk; jwcai@iphy.ac.cn; yongbing.xu@york.ac.uk

Abstract

Ultrathin CoFeB-based magnetic tunnel junction (MTJ) is the key for the next generation magnetic random-access memory (MRAM). However, the underlying mechanism of the perpendicular magnetic anisotropy (PMA) in Ta/CoFeB/MgO structure is still unclear. Herein, the PMA in the Ta/CoFeB/MgO system has been studied using X-ray magnetic circular dichroism and vibrating sample magnetometry. The ratios of the orbital to spin magnetic moments of Co atoms in the Ta/CoFeB/MgO structures with PMA have been found to be enhanced by 100%, compared with the Ta/CoFeB/Ta structure without PMA. The orbital moments of Co are as large as $0.30\,\mu_B$, more than half of their spin moments in the perpendicularly magnetised Ta/CoFeB/MgO structures. The results indicate that the PMA observed in the Ta/CoFeB/MgO structures is related to the increased spin-orbital coupling of the Co atoms. This work offers experimental evidence of the correlation between PMA and the element specific spin and orbital moments in the Ta/CoFeB/MgO systems.

Keywords

CoFeB thin film, PMA, XMCD, orbital moments

1 Introduction

Spintronic devices, which exploit the exchange interaction of the electron spins, are strong candidates for non-volatile memory due to the inherent hysteresis in the ferromagnetic materials and the compatibility with the complementary metal-oxide-semiconductor (CMOS) process.[1,2] Magnetoresistive random access memory (MRAM) has exhibited significant advantages as a fast, fairly low-power, high-endurance, radiation-resistant and non-volatile memory, which can be integrated to the CMOS as a back-end of line (BEOL) process.[3] The read-out process of the MRAM bits is reliably performed via the tunneling magnetoresistance (TMR) effect[4–7] in magnetic tunnel junctions (MTJs). A major breakthrough in

MRAM is the discovery of perpendicularly magnetised CoFeB films, sandwiched by MgO and Ta layers, which exhibit not only the perpendicular magnetic anisotropy, but also strong orbital moment and spin-orbital coupling.[8] The perpendicular magnetic anisotropy (PMA) materials, integrated into a MTJ,[9–14] allow for a small critical current density for current-induced magnetisation switching.[15–17] CoFeB is now the most studied material system for MTJ structures due to its high MR value[18] and low Gilbert damping.[19] The value of TMR effect has been reported as high as 138% $\sim$ 604%[18,20–22] in the CoFeB/MgO/CoFeB pseudo-spin-valve MTJ. The key to achieve a perpendicular-anisotropy CoFeB/MgO MTJ is the very thin thickness of CoFeB layer.[23,24] The PMA was attributed entirely to the CoFeB-MgO interfacial anisotropy by Ikeda *et al.*,[8] while the Ta seed layer, not just the MgO at the top interface, was demonstrated to be critical to achieving perpendicular magnetic anisotropy.[25] The microscopic origin of the PMA in the CoFeB/MgO structure is still far from clear. In this work, we report the effect of the layered structure and in particularly the role of the element-specific orbital moments on the PMA in the Ta/CoFeB/MgO structures.

2 Experimental section

Three different layered samples were prepared as shown in Figure 1. Sample A has a structure of substrate/Ta(5)/MgO(3)/CoFeB(1.2)/Ta(5), where the numbers denote the thickness of each layer in nanometers. Sample B and C have structures of substrate/Ta(5)/CoFeB(1.2)/MgO(3)/CoFeB(and substrate/Ta(5)/CoFeB(1.2)/Ta(5), respectively. All the three samples were deposited on Si(001)/SiO_2 substrates. The Ta layer was deposited by direct current (DC) sputtering, whereas the MgO and $Co_{40}Fe_{40}B_{20}$ layers were deposited using radio frequency (RF) sputtering. The base pressure of growth chamber was under 4×10^{-5} Pa and the working argon pressure was 0.5 Pa. After the films were deposited, a post-annealing process at 300 °C in a vacuum chamber at 4×10^{-5} Pa, was performed for 30 min on all the samples.

The magnetic hysteresis loops were measured with both the in-plane and perpendicular

magnetic fields using vibrating sample magnetometer (VSM, ADE, Model 10). The maximum magnetic field of 1.5 T was applied to ensure the samples were saturated. X-ray absorption spectroscopy (XAS) and X-ray magnetic circular dichroism (XMCD) at the Fe and Co $L_{2,3}$ edges were performed in the beamline I06 at the Diamond Light Source. The total-electron yield (TEY) was monitored using the sample drain current. Circularly polarized X-ray with 100% polarization degree incidents to the samples at an angle of 30° with respect to the sample normal, and a magnetic field of 2 T were applied perpendicular to the incident beam. The magnitude of the XMCD asymmetry was obtained via $\mu_+ - \mu_-/(\mu_+ + \mu_-)$, where $\mu_{-,+}$ represents the XAS intensity for both helicities of the X-ray beam. All the XMCD measurements were performed at room temperature.

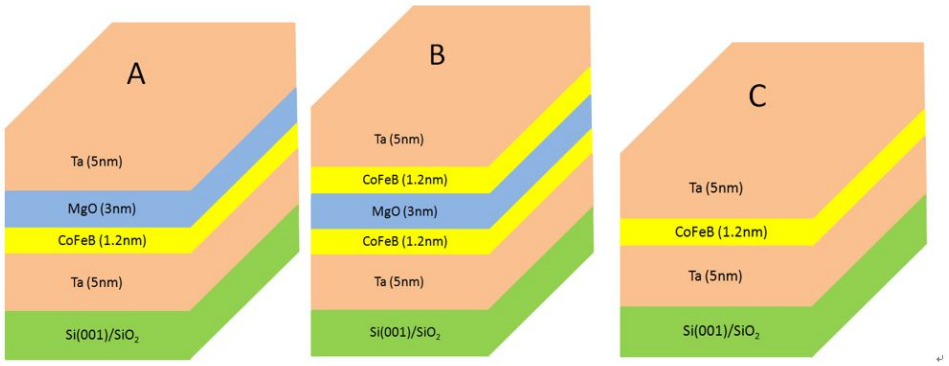

Figure 1: Stack structures of three samples. Sample A: Ta(5nm)/MgO(3nm)/CoFeB(1.2nm)/Ta(5nm)/Substrate, sample B: Ta(5nm)/CoFeB(1.2nm)/MgO(3nm)/CoFeB(1.2nm)/Ta(5nm)/Substrate and sample C: Ta(5nm)/CoFeB(1.2nm)/Ta(5nm)/Substrate.

3 Results and discussion

Figure 2 shows the magnetic hysteresis loops of all the samples with both in-plane and perpendicular applied magnetic fields. The PMA is observed in both sample A and B: the in-plane loops show the magnetic hard axis while the out-of-plane loops show the magnetic easy axis. However, the PMA is not observed in sample C, the film without the MgO layer, where the in-plane loop represents the magnetic hard axis. The saturation fields along the

hard axis of sample A, B (in-plane), and C (out-of-plane) are around 6500 Oe, 7000 Oe, and 13 000 Oe, respectively. The effective magnetic anisotropy constant K_u^{eff} can be calculated using the following equation:[26,27]

$$K_u^{eff} = \frac{H_K \cdot M_s}{2} \tag{1}$$

where H_k is the saturation magnetic field along hard axis and M_s is the saturation magnetisation.

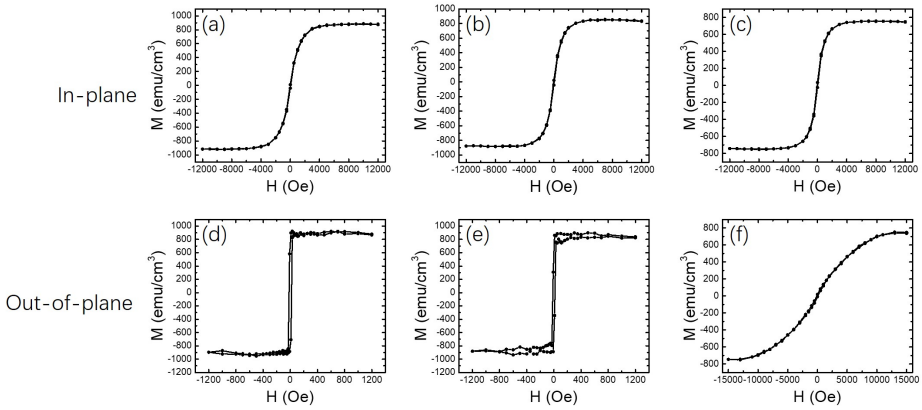

Figure 2: In-plane (up row) and out-of-plane (bottom row) hysteresis loops of sample A (Ta(5nm)/MgO(3nm)/CoFeB(1.2nm)/Ta(5nm)/Substrate): (a), (d); B (Ta(5nm)/CoFeB(1.2nm)/MgO(3nm)/CoFeB(1.2nm)/Ta(5nm)/Substrate): (b), (e); and C (Ta(5nm)/CoFeB(1.2nm)/Ta(5nm)/Substrate): (c), (f), respectively.

Table 1: The values of the saturation fields along magnetic hard axis, the saturation magnetisation, and the effective magnetic anisotropy constant of sample A, B, and C.

Sample	H_k(Oe)	M_s(emu/cm^3)	K_u^{eff}(Merg/cm^3)
A: Ta/MgO/CoFeB/Ta	6500 (in-plane)	875	+2.84
B: Ta/CoFeB/MgO/CoFeB/Ta	7000 (in-plane)	830	+2.91
C: Ta/CoFeB/Ta	13000 (out-of-plane)	743	−4.83

Shown in Table 1, the values of the saturation field along magnetic hard axis and the saturation magnetisation of sample A are 6500 Oe and 875 emu/cm^3, respectively, which are very similar to the reported study,[28,29] while the effective magnetic anisotropy constant of 2.84 Merg/cm^3 is much larger showing a strong PMA. In sample B, it is very interesting

that the PMA is observed with a total thickness of CoFeB of 2.4 nm, exceeding the thickness limitation of 1.2 nm to form PMA.[30] When the CoFeB layer is divided into two layers of 1.2 nm thickness with the MgO layer, the PMA presents. It can be found that the values of H_k, M_s and K_u^{eff} of samples A and B are in a similar level: H_k and K_u^{eff} of sample A are slightly smaller than those of sample B while M_s of sample A is slightly larger than sample B. This observation suggests that a $[\mathrm{Ta/CoFeB/MgO/CoFeB}]_n$ multilayer structure could possibly have PMA if the CoFeB layer is of proper thickness. It should be noted that the value of K_u^{eff} for sample C is presented as the negative value because sample C doesn't form a PMA.

The measured XAS of both Co and Fe at L_2 and L_3 edges for all the samples are shown in Figure 3, in which μ_+ and μ_- represent the absorption coefficients under antiparallel and parallel magnetic fields to the photo incident direction. Figure 3 also shows the XMCD spectra of both Co and Fe at L-edges. Figure 3(a), (c) and (e) are the Co element XMCD diagrams, where the L_3 photon energy of Co is around 778.4 eV. Figure 3(b), (d) and (f) give the XMCD diagrams for Fe, where the L_3 photon energy of Fe is around 707.4 eV. According to the XMCD sum rules, orbital magnetic moments (m_{orb}), spin magnetic moments (m_{spin}), and orbital to spin moment ratio (m_{ratio}) can be determined from XAS and XMCD spectra by the sum rules:[31–34]

$$\begin{aligned} m_{orb} &= -\frac{4\int_{L_2+L_3}(\mu_+-\mu_-)d\omega}{3\int_{L_2+L_3}(\mu_++\mu_-)d\omega}(10-n_{3d}) \\ m_{spin} &= -\frac{6\int_{L_3}(\mu_+-\mu_-)d\omega-4\int_{L_3+L_2}(\mu_+-\mu_-)d\omega}{\int_{L_2+L_3}(\mu_++\mu_-)d\omega} \times \frac{(10-n_{3d})}{(1+\frac{7\langle T_z\rangle}{2\langle S_z\rangle})} \\ m_{ratio} &= \frac{m_{orb}}{m_{spin}} \end{aligned} \tag{2}$$

where the magnetic moments are in units of μ_B/atom; n_{3d} is the 3d electron occupation number of the respective transition metal atom; L_3 and L_2 denote the integration range; $\langle T_z\rangle$ is the expectation value of the magnetic dipole operator and $\langle S_z\rangle$ is equal to half of m_{spin} in Hartree atomic units.

It should be noted that there is a degree of controversy regarding the 3d hole numbers

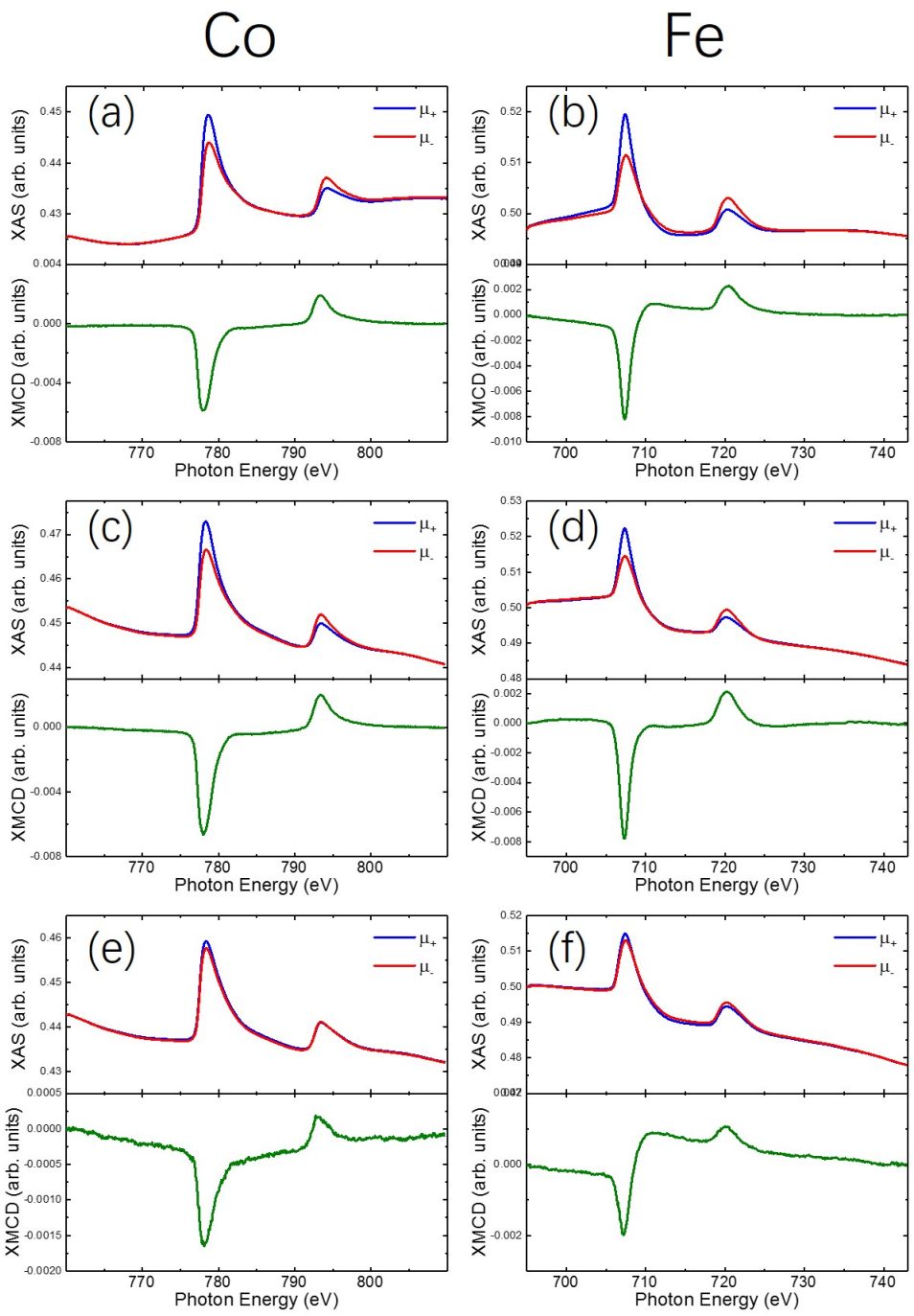

Figure 3: XAS and XMCD spectra of the Co (left column) and Fe (right column) atoms at the L_2 and L_3 edges in the sample A (Ta(5nm)/MgO(3nm)/CoFeB(1.2nm)/Ta(5nm)/Substrate): (a) and (b), sample B (Ta(5nm)/CoFeB(1.2nm)/MgO(3nm)/CoFeB(1.2nm)/Ta(5nm)/Substrate): (c) and (d), and sample C (Ta(5nm)/CoFeB(1.2nm)/Ta(5nm)/Substrate): (e) and (f).

of Fe and Co in magnetic amorphous films. While Cui *et al.*[35] use the m_{orb}/n_h to present their data, Kainai *et al.*[30] have calculated the hole numbers of Co and Fe in the amorphous films by first-principles calculations, and have found the similar values to those of the bulk Fe and Co films.[29,30] In this work, we have used the values of n_{3d} for Fe as 6.61 and Co as 7.51, taken from,[36] to calculate the spin and orbital moments of Co and Fe in the CoFeB films.

The values of m_{orb}, m_{spin} and m_{ratio} are all determined from the XMCD data, and the results are listed in Table 2, along with some reported values in the literature. By drawing a comparison between the films with a MgO layer (A and B) forming the PMA and the film with neither a MgO layer (C) nor a PMA, it is demonstrated that the orbital moments of Fe and Co elements in sample A and B (with a MgO layer) are larger than those of sample C (without a MgO layer). This observation is especially pronounced in the orbital moment of Co, showing a nearly 100% enhancement in sample A and B compared to sample C. On the other hand, the spin moments of both Co and Fe in the three samples do not show such dramatic differences. The values of m_{spin} are around 1.65 μ_B for Fe and 0.59 μ_B for Co.

Table 2: Orbital moments, spin moments and orbital to spin ratio of the Fe and Co from various CoFeB samples

Sample	Element	$m_{orb}(\mu_B)$	$m_{spin}(\mu_B)$	$m_{total}(\mu_B)$	m_{ratio}
A: Ta/MgO/CoFeB(1.2 nm)/Ta	Fe	0.31 ± 0.02	1.69 ± 0.02	2.00 ± 0.04	0.19
	Co	0.30 ± 0.04	0.59 ± 0.01	0.89 ± 0.05	0.52
B: Ta/CoFeB(1.2 nm)/MgO/CoFeB(1.2 nm)/Ta	Fe	0.26 ± 0.03	1.61 ± 0.03	1.87 ± 0.06	0.16
	Co	0.30 ± 0.01	0.58 ± 0.02	0.88 ± 0.03	0.51
C: Ta/CoFeB(1.2 nm)/Ta	Fe	0.20 ± 0.04	1.68 ± 0.02	1.88 ± 0.06	0.12
	Co	0.17 ± 0.05	0.60 ± 0.03	0.77 ± 0.08	0.28
Ta/CoFeB(2.0 nm)/MgO/Ta[30]	Fe	0.27 ± 0.03	1.77 ± 0.03	2.04 ± 0.06	0.15
	Co	0.17 ± 0.03	0.90 ± 0.03	1.07 ± 0.06	0.19
Bulk bcc Fe[35,36]	Fe	0.09 ± 0.05	1.98 ± 0.05	2.07 ± 0.10	0.04
Bulk hcp Co[35,36]	Co	0.15 ± 0.05	1.55 ± 0.05	1.70 ± 0.10	0.10

[a] CoFeB denotes $Co_{40}Fe_{40}B_{20}$.

Although a CoFeB layer with a thickness thicker than 1.2 nm would not be able to form the PMA, in this work the total thickness of CoFeB layers (two layers) in sample B was

2.4 nm, which presents the PMA. By comparing the value of magnetic moments of sample A and B with the values in Ref. 30, it can be seen that the orbital moments of Fe have not dramatically changed, but the orbital moments of Co have increased from 0.17 μ_B to 0.30 μ_B. It should be noted that the value of the Co orbital moment in Ref. 30 is 0.17 μ_B, which is the same as the value from sample C while neither of these two samples have the PMA. Compared to the sample C, by replacing the Ta layer by the MgO layer in Ref. 30, only the orbital moment of Fe slightly increased, but the orbital moment of Co is of the same value. Therefore, our results suggest that the enhancement of Co orbital moments is associated with the origin of PMA in the CoFeB/MgO system.

Spin-orbital coupling is a desired property in terms of the ability to use an electric field to control spintronic operation. One of the most striking results from the measurements (as shown in Table 2) is that the orbital moments and m_{ratio} of Co atoms are significantly larger than those of Fe atoms. This suggests Co atoms at the interface with MgO contribute more than Fe atoms in spin-orbital coupling. The spin to orbital ratio of Co atoms in samples A and B (which present the PMA) is 0.52, showing a nearly 100% enhancement compared to the values of sample C and in Ref. 30 which did not form the PMA. The spin to orbital ratios of Fe, however have not shown significant change in all the samples. It is suggested that the strong PMA in the CoFeB/MgO system is related to the large enhancement of the orbital moment of Co element rather than Fe. This is consistent with the observations in the CoFeB/GaAs system, where the strong in-plane uniaxial magnetic anisotropy was demonstrated to be related to the enhanced orbital moment of Co.[27]

4 Conclusion

In summary, we have systematically investigated perpendicular magnetic anisotropy and the element specific spin and orbital moments in the CoFeB/MgO system. The results obtained from VSM measurements confirmed that the PMA can be formed in a split CoFeB

layers of a total thickness of 2.4 nm, with a MgO interlayer. and the saturation field along hard axis (in-plane) can be as high as 7000 Oe, which enhanced 10% compared to the sample Ta(5)/MgO(3)/CoFeB(1.2)/Ta(5), while the M_s and K_u^{eff} are at the similar level. XMCD measurements revealed that the PMA is correlated with the strong spin-orbital coupling of Co atoms, related to the enhanced orbital to spin moment ratios of Co atoms in CoFeB. More importantly, compared with the samples without PMA (sample C: Ta(5)/CoFeB(1.2)/Ta(5) and Ta(5)/CoFeB(1.2)/Ta(5) from Ref. 30), the samples with the PMA (sample A: Ta(5)/MgO(3)/CoFeB(1.2)/Ta(5) and sample B: Ta(5)/CoFeB(1.2)/MgO(3)/CoFeB(1.2) show the orbital moment of Co atoms enhanced from 0.17 μ_B to 0.30 μ_B. Meanwhile, the orbital moment of Fe atoms has not shown significant change, suggesting the dominant contribution of spin-orbital moment coupling of Co atoms to the PMA in CoFeB/MgO structures. These results provide insight into the origin of the PMA in the Ta/CoFeB/MgO films, which is important for the development of spintronic memory devices like STT-MRAM.

Acknowledgement

This work was supported in part by the National Basic Research Program of China (No. 2014CB921101), National Key Research and Development Program of China (No. 2016YFA0300803), the National Natural Science Foundation of China (No. 61427812, 11574137, 11774160, 51871236), Jiangsu Shuangchuang Programme, the Natural Science Foundation of Jiangsu Province of China (No. BK20140054) and UK EPSRC EP/S010246/1. Diamond Light Source is acknowledged to I10 under proposal No. 16538.

References

(1) Assefa, S.; Nowak, J.; Sun, J. Z.; O'Sullivan, E.; Kanakasabapathy, S.; Gallagher, W. J.; Nagamine, Y.; Tsunekawa, K.; Djayaprawira, D. D.; Watanabe, N. Fabrication and

characterization of MgO-based magnetic tunnel junctions for spin momentum transfer switching. *J. Appl. Phys.* **2007**, *102*.

(2) Huai, Y.; Albert, F.; Nguyen, P.; Pakala, M.; Valet, T. Observation of spin-transfer switching in deep submicron-sized and low-resistance magnetic tunnel junctions. *Appl. Phys. Lett.* **2004**, *84*, 3118–3120.

(3) Chen, E. et al. Advances and Future Prospects of Spin-Transfer Torque Random Access Memory. *IEEE Trans. Magn.* **2010**, *46*, 1873–1878.

(4) Katine, J. A.; Albert, F. J.; Buhrman, R. A.; Myers, E. B.; Ralph, D. C. Current-driven magnetization reversal and spin-wave excitations in Co/Cu/Co pillars. *Phys. Rev. Lett.* **2000**, *84*, 3149–3152.

(5) Parkin, S. S.; Kaiser, C.; Panchula, A.; Rice, P. M.; Hughes, B.; Samant, M.; Yang, S. H. Giant tunnelling magnetoresistance at room temperature with MgO (100) tunnel barriers. *Nat. Mater.* **2004**, *3*, 862–7.

(6) Wang, J.; Zhang, X.; Lu, X.; Zhang, J.; Yan, Y.; Ling, H.; Wu, J.; Zhou, Y.; Xu, Y. Magnetic domain wall engineering in a nanoscale permalloy junction. *Appl. Phys. Lett.* **2017**, *111*, 072401.

(7) Singh, A. K.; Eom, J. Negative magnetoresistance in a vertical single-layer graphene spin valve at room temperature. *ACS Appl. Mater. Interfaces* **2014**, *6*, 2493–6.

(8) Ikeda, S.; Miura, K.; Yamamoto, H.; Mizunuma, K.; Gan, H. D.; Endo, M.; Kanai, S.; Hayakawa, J.; Matsukura, F.; Ohno, H. A perpendicular-anisotropy CoFeB-MgO magnetic tunnel junction. *Nat. Mater.* **2010**, *9*, 721–4.

(9) Teixeira, J. M.; Silva, R. F. A.; Ventura, J.; Pereira, A. M.; Carpinteiro, F.; Araújo, J. P.; Sousa, J. B.; Cardoso, S.; Ferreira, R.; Freitas, P. P. Domain imag-

ing, MOKE and magnetoresistance studies of CoFeB films for MRAM applications. *Mater. Sci. Eng. B* **2006**, *126*, 180–186.

(10) Zhu, T.; Chen, P.; Zhang, Q. H.; Yu, R. C.; Liu, B. G. Giant linear anomalous Hall effect in the perpendicular CoFeB thin films. *Appl. Phys. Lett.* **2014**, *104*, 202404.

(11) Liu, T.; Zhang, Y.; Cai, J. W.; Pan, H. Y. Thermally robust Mo/CoFeB/MgO trilayers with strong perpendicular magnetic anisotropy. *Sci. Rep.* **2014**, *4*, 5895.

(12) Barati, E.; Cinal, M.; Edwards, D. M.; Umerski, A. Gilbert damping in magnetic layered systems. *Phys. Rev. B* **2014**, *90*, 014420.

(13) Sato, H.; Enobio, E. C. I.; Yamanouchi, M.; Ikeda, S.; Fukami, S.; Kanai, S.; Matsukura, F.; Ohno, H. Properties of magnetic tunnel junctions with a MgO/CoFeB/Ta/CoFeB/MgO recording structure down to junction diameter of 11 nm. *Appl. Phys. Lett.* **2014**, *105*, 062403.

(14) Ko, J.; Hong, J. Voltage-Assisted Magnetic Switching in MgO/CoFeB-Based Magnetic Tunnel Junctions by Way of Interface Reconstruction. *ACS Appl. Mater. Interfaces* **2017**, *9*, 42296–42301.

(15) Brataas, A.; Kent, A. D.; Ohno, H. Current-induced torques in magnetic materials. *Nat. Mater.* **2012**, *11*, 372–81.

(16) Zhu, T.; Yang, Y.; Yu, R. C.; Ambaye, H.; Lauter, V.; Xiao, J. Q. The study of perpendicular magnetic anisotropy in CoFeB sandwiched by MgO and tantalum layers using polarized neutron reflectometry. *Appl. Phys. Lett.* **2012**, *100*, 202406.

(17) Yoshikawa, M.; Kitagawa, E.; Nagase, T.; Daibou, T.; Nagamine, M.; Nishiyama, K.; Kishi, T.; Yoda, H. Tunnel Magnetoresistance Over 100% in MgO-Based Magnetic Tunnel Junction Films With Perpendicular Magnetic $L1_0$-FePt Electrodes. *IEEE Trans. Magn.* **2008**, *44*, 2573–2576.

(18) Ikeda, S.; Hayakawa, J.; Ashizawa, Y.; Lee, Y. M.; Miura, K.; Hasegawa, H.; Tsunoda, M.; Matsukura, F.; Ohno, H. Tunnel magnetoresistance of 604% at 300 K by suppression of Ta diffusion in CoFeB/MgO/CoFeB pseudo-spin-valves annealed at high temperature. *Appl. Phys. Lett.* **2008**, *93*, 082508.

(19) Liu, B.; Ruan, X.; Wu, Z.; Tu, H.; Du, J.; Wu, J.; Lu, X.; He, L.; Zhang, R.; Xu, Y. Transient enhancement of magnetization damping in CoFeB film via pulsed laser excitation. *Appl. Phys. Lett.* **2016**, *109*, 042401.

(20) Djayaprawira, D. D.; Tsunekawa, K.; Nagai, M.; Maehara, H.; Yamagata, S.; Watanabe, N.; Yuasa, S.; Suzuki, Y.; Ando, K. 230% room-temperature magnetoresistance in CoFeB/MgO/CoFeB magnetic tunnel junctions. *Appl. Phys. Lett.* **2005**, *86*, 092502.

(21) Cha, J. J.; Read, J. C.; Egelhoff, W. F.; Huang, P. Y.; Tseng, H. W.; Li, Y.; Buhrman, R. A.; Muller, D. A. Atomic-scale spectroscopic imaging of CoFeB/Mg-B-O/CoFeB magnetic tunnel junctions. *Appl. Phys. Lett.* **2009**, *95*, 032506.

(22) Tsunekawa, K.; Djayaprawira, D. D.; Nagai, M.; Maehara, H.; Yamagata, S.; Watanabe, N.; Yuasa, S.; Suzuki, Y.; Ando, K. Giant tunneling magnetoresistance effect in low-resistance CoFeB/MgO(001)/CoFeB magnetic tunnel junctions for read-head applications. *Appl. Phys. Lett.* **2005**, *87*, 072503.

(23) Liu, Y.; Zhang, J.; Wang, S.; Jiang, S.; Liu, Q.; Li, X.; Wu, Z.; Yu, G. Ru Catalyst-Induced Perpendicular Magnetic Anisotropy in MgO/CoFeB/Ta/MgO Multilayered Films. *ACS Appl. Mater. Interfaces* **2015**, *7*, 26643–8.

(24) Qin, Z.; Wang, Y.; Zhu, S.; Jin, C.; Fu, J.; Liu, Q.; Cao, J. Stabilization and Reversal of Skyrmion Lattice in Ta/CoFeB/MgO Multilayers. *ACS Appl. Mater. Interfaces* **2018**, *10*, 36556–36563.

(25) Worledge, D. C.; Hu, G.; Abraham, D. W.; Sun, J. Z.; Trouilloud, P. L.; Nowak, J.; Brown, S.; Gaidis, M. C.; O'Sullivan, E. J.; Robertazzi, R. P. Spin torque switching

of perpendicular Ta|CoFeB|MgO-based magnetic tunnel junctions. *Appl. Phys. Lett.* **2011**, *98*, 022501.

(26) Wastlbauer, G.; Bland, J. A. C. Structural and magnetic properties of ultrathin epitaxial Fe films on GaAs(001) and related semiconductor substrates. *Adv. Phys.* **2005**, *54*, 137–219.

(27) Yan, Y. et al. Element specific spin and orbital moments of nanoscale CoFeB amorphous thin films on GaAs(100). *AIP Adv.* **2016**, *6*, 095011.

(28) Liu, B.; Huang, D.; Gao, M.; Tu, H.; Wang, K.; Ruan, X.; Du, J.; Cai, J.-W.; He, L.; Wu, J.; Wang, X.; Xu, Y. The effect of growth sequence on magnetization damping in Ta/CoFeB/MgO structures. *J. Magn. Magn. Mater.* **2018**, *450*, 65–69.

(29) Ueno, T.; Sinha, J.; Inami, N.; Takeichi, Y.; Mitani, S.; Ono, K.; Hayashi, M. Enhanced orbital magnetic moments in magnetic heterostructures with interface perpendicular magnetic anisotropy. *Sci. Rep.* **2015**, *5*, 14858.

(30) Kanai, S.; Tsujikawa, M.; Miura, Y.; Shirai, M.; Matsukura, F.; Ohno, H. Magnetic anisotropy in Ta/CoFeB/MgO investigated by x-ray magnetic circular dichroism and first-principles calculation. *Appl. Phys. Lett.* **2014**, *105*, 222409.

(31) Chen, C. T.; Idzerda, Y. U.; Lin, H.; Smith, N. V.; Meigs, G.; Chaban, E.; Ho, G. H.; Pellegrin, E.; Sette, F. Experimental confirmation of the X-ray magnetic circular dichroism sum rules for iron and cobalt. *Phys. Rev. Lett.* **1995**, *75*, 152–155.

(32) Liu, W.; Zhou, Q.; Chen, Q.; Niu, D.; Zhou, Y.; Xu, Y.; Zhang, R.; Wang, J.; van der Laan, G. Probing the buried magnetic interfaces. *ACS Appl. Mater. Interfaces* **2016**, *8*, 5752–5757.

(33) Liu, W.; Wang, W.; Wang, J.; Wang, F.; Lu, C.; Jin, F.; Zhang, A.; Zhang, Q.;

Van Der Laan, G.; Xu, Y.; Li, Q.; Zhang, R. Atomic-scale interfacial magnetism in Fe/graphene heterojunction. *Sci. Rep.* **2015**, *5*, 11911.

(34) Huang, Z.; Liu, W.; Yue, J.; Zhou, Q.; Zhang, W.; Lu, Y.; Sui, Y.; Zhai, Y.; Chen, Q.; Dong, S.; Wang, J.; Xu, Y.; Wang, B. Enhancing the Spin-Orbit Coupling in Fe3O4 Epitaxial Thin Films by Interface Engineering. *ACS Appl. Mater. Interfaces* **2016**, *8*, 27353–27359.

(35) Cui, B.; Song, C.; Wang, Y. Y.; Yan, W. S.; Zeng, F.; Pan, F. Tuning of uniaxial magnetic anisotropy in amorphous CoFeB films. *J. Phys.: Condens. Matter* **2013**, *25*, 106003.

(36) Chen, C. T.; Idzerda, Y. U.; Lin, H. J.; Meigs, G.; Chaiken, A.; Prinz, G. A.; Ho, G. H. Element-specific magnetic hysteresis as a means for studying heteromagnetic multilayers. *Phys. Rev. B* **1993**, *48*, 642–645.